RSC Advances

ROYAL SOCIETY OF CHEMISTRY

www.rsc.org/advances

Graphical Abstract

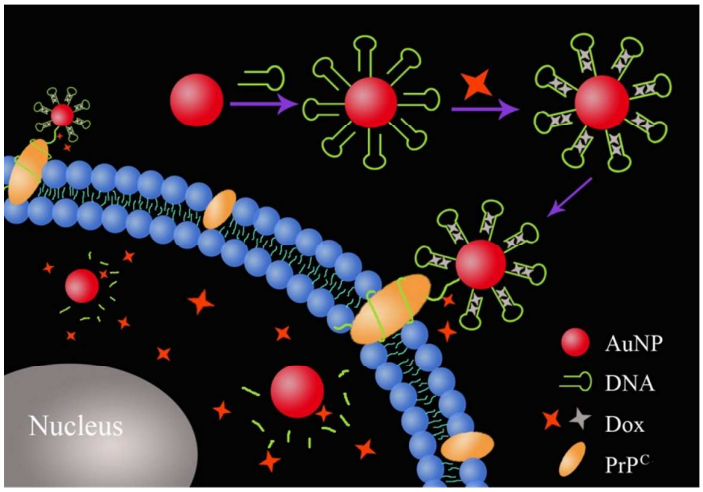

A targeting drug delivery system that based on AuNPs and DNA was developed to treat neuroblastoma cancer, which exhibits excellent specificity in delivering and releasing of doxorubicin, and has great prospects in clinical applications.

Cite this: DOI: 10.1039/c0xx00000x

www.rsc.org/xxxxxx

ARTICLE TYPE

A cancer-targeted drug delivery system developed with gold nanoparticles mediated DNA-doxorubicin conjugates

Yu Qing Du,[a] Xiao Xi Yang,[a] Wen Long Li,[b] Jian Wang*,[a] and Cheng Zhi Huang*[a]

Received (in XXX, XXX) Xth XXXXXXXXX 20XX, Accepted Xth XXXXXXXXX 20XX

DOI: 10.1039/b000000x

Clinic therapies of cancers are generally unsatisfactory with poor patient compliance because of low therapeutic efficiency and strong side effects in normal tissues. To overcome these shortcomings and improve the efficacy of medicine, it is necessary to design some new targeting ligands, in comparable to the folic acid ligand commonly used. Here we report a new drug delivery system for targeted therapy of neuroblastoma cancer by functionalizing the surface of gold nanoparticle (AuNPs) with DNA that contains cellular prion protein (PrP^C) aptamer. Owing to the specific identification between aptamer and PrP^C expressed on the surface of the human bone marrow neuroblastoma (SK-N-SH) cells, the DNA-drug conjugates could be delivered to the target cancer cells and thus apoptosis of these cells occurred. The vitro toxicity assay and fluorescence imaging results showed that the AuNPs mediated DNA-doxorubicin conjugates (AuNPs-DNA(Dox)) could be demonstrated as a specific and effective therapeutic agent for neuroblastoma cancer.

Introduction

Cancers are considered to be the most serious illnesses in the world, which cause millions of deaths every year.[1] Chemotherapy and radiotherapy are still the standard treatments after surgical resection of the tumor sites, and they are only employed to prolong life or alleviate symptoms temporarily. Both methods make patients uncomfortable, and even some people can't tolerate the pain so that they give up treatment finally. Moreover, current chemotherapeutic agents enter the bloodstream, and then distribute into both cancer cells and normal cells, which are lack of specificity and so that lead to undesirable side effects to normal tissues during therapy.[2] To avoid the complex side effect and improve patient compliance, controlling the release of drug[3, 4] and developing effective targeting platforms[5] for cancer therapy are very necessary.

Up to 2009, there had been 36 countries approved the paclitaxel-albumin nanoparticle as an anti-tumor drug used in clinical treatment of breast cancer,[6, 7] which indicated that nanomaterials-based drug delivery systems have great potential application in clinic. Nano-materials, due to their biocompatibility, lower toxicity, unique optical and electrical properties, have become hot topics in targeting drug carrier research.[8-13] Recently, a pH-responsive polymer sphere as vehicle for drug delivery targeted to folic acid receptor on the surface of cancer cells has been developed in our group.[14] Based on folate receptor-mediated mechanisms, other nanomaterials such as AuNPs,[15] mesoporous silica[16] and graphene oxide[17] were also used to selectively and effectively deliver drugs. Except folate receptor, other targeting ligands, like protein,[18-20] peptide[21, 22], and target gene[23] have received considerable attention in drug delivery, and have achieved ideal therapy effect. On the other hand, aptamer, which is a single-stranded oligonucleotides that could specifically recognize various kinds of targets such as proteins, drug molecules and cancer cells,[24] has the advantages of excellent specificity, low toxicity, high affinity and easy to be synthesized, modified and manipulated, and thus has been widely investigated for drug delivery[25] and cancer cells detection[26].

Neuroblastoma is a serious cancer that 96% occurs before the age of 10 years, and SK-N-SH cells is one of the cancer cell lines in human neuroblastoma.[27] Developing a drug delivery system that targeted to SK-N-SH cells would have great significance for the treatment of neuroblastorma. PrP^C is one of the membrane protein that expressed on the SK-N-SH cells and has an aptamer can bind with the 23-90 epitope.[26] The specific identification between aptamer and PrP^C have been widely employed in biochemical detection[28] and biological imaging[29]. Considering that Dox is a cancer treatment drugs that can intercalate in the stem double-stranded CG or GC sequence of DNA[30], herein we designed a DNA fragment that contains aptamer and double-stranded CG sequences as both a recognizer for target protein on cancer cells and a carrier for the delivery of Dox, and thus developed a novel and effective strategy for targeted deliver Dox to SK-N-SH cells based on the identification of aptamer and PrP^C. Although Dox has been used for clinical treatment of many common human cancers such as breast cancer, prostate cancer and neuroblastoma cancer.[30, 31] the widely clinical application of Dox is still limited by the side effects of nonspecific delivery and poor release of drug into target tumor sites. To aviod those bad aspects, AuNPs and DNA were chosen to targeted deliver drug. The vitro toxicity assay and fluorescence imaging results showed that the AuNPs-DNA(Dox) conjugates can effectively deliver drug to target cells and induce them apoptosis.

Experimental Section

Apparatus

Fluorescence and absorption spectra were measured by using a F-2500 fluorescence spectrophotometer (Hitachi, Tokyo, Japan) and a U-3600 spectrophotometer (Hitachi, Tokyo, Japan), respectively. A vortex mixer, OL-901 (Haimen, China), was employed to blend the solution. Fluorescence imaging was performed with an IX81 microscope (Olympus, Japan). Dynamic light scattering (DLS) measurements were carried out with a Malvern Nano-ZS Zetasizer. The size and shape of AuNPs were observed through S-4800 scanning electron microscope (SEM, Hitachi, Japan).

Materials

DNA (5'-SH-TTT CGA CGA CTT ACG GTG GGG CAA TTT CGT CG-3', the underline part was the aptamer of PrP^C) was synthesized by Sangon Biotechnology Co., Ltd. (Shanghai, China). Chloroauric acid ($HAuCl_4{\cdot}4H_2O$) was purchased from Sinopharm Group Chemical Reagent Co. Ltd. (Shanghai, China). Tris (2-carboxyethyl) phosphine hydrochloride (TCEP) was gained from Sigma-Aldrich (Missouri, USA). Trisodium citrate ($Na_3C_6H_5O_7{\cdot}2H_2O$) was supplied by the Chemical Reagent Co. (Shanghai, China). Doxorubicin hydrochloride (Dox·HCl) was obtained from Melone Pharmaceutical Co., Ltd (Dalian, China). All the reagents were used without further purification. Mili-O purified water (18.2 MΩ) was used in the entire experiment.

Expression of recombinant human prion protein

In this work, according to the reported method,[26] the plasmid encoading recombinant human prion protein (23-231) was transformed to *Escherichia coli* BL21-DE3. The bacteria were cultured overnight in lysogeny broth (LB) medium with kanamycin (Sigma), and then transferred into 2 × YT medium with 1 % inoculation volume, and induced by isopropyl β-D-1-thiogalactopyranoside (IPTG) (Sigma) for 6 h expression, then the protein were harvested and purificated with nickel-nitrilotriacetic acid (NTA) agarose resin (Invitrogen, Germany). The concentration of the prion protein was determined by absorption spectrum.

Prepare of citrate capped 13 nm gold nanoparticles

13 nm gold nanoparticles (AuNPs) were synthesized as reported.[32] All glassware used was thoroughly cleaned using aqua regia solution (HCl/HNO_3 in volume = 3: 1) before use. In a 100 mL flat-bottomed flask with a condenser, the mixture of 50 mL ultra-pure water and 2 mL 1% $HAuCl_4{\cdot}4H_2O$ was heated to boiling with vigorous stirring. Then 1 mL 5 % trisodium citrate was added quickly, which resulted in color changes from pale yellow to dark-blue and then to fresh red. The solution was kept boiling for another 10 min to ensure completed reduction, then cooled down to room temperature under continuous stirring. The size of AuNPs was verified by SEM and dynamic light scattering, and their concentration was estimated by UV-vis spectroscopy.

Conjugation of DNA with AuNPs

The DNA-modified AuNPs were prepared as follows.[33, 34] Firstly, thiol-modified DNA was activated by 100 μL 100 μM TCEP for 1 h. Then, TCEP-activated DNA was incubated with AuNPs at room temperature. After 16 h, 100 mM NaCl was added through a gently shaken process. The mixture was further incubated for 24 h at room temperature. Next, the excess DNA was removed by centrifugation at 15000 rpm for 20 min, and the precipitate was washed twice with repetitive centrifugation and dispersion, which was finally dispersed in the buffer (10 mM Tris-HCl, pH 8.0, 100 mM KCl, 1 mM $MgCl_2$) and stored at 4 °C for the next experiment.

Reaction between DNA and Dox

According to previous reports,[35] the anthracycline class of drugs, like Dox, displays fluorescence property that could be quenched by intercalating into the double-stranded 5'-GC-3' or 5'-CG-3' base pairs of DNA. To study the reaction stoichiometry between DNA and Dox, a fixed concentration of Dox (200 nM) was incubated with an increasing concentration of DNA (0, 20, 40, 60, 80, 100, 120 nM) for 1 h, then the fluorescence spectrum of the mixture was measured at 490 nm excitation.

Dox loading to AuNPs-DNA

DNA conjugated AuNPs (2 nM) were incubated with Dox (1 μM) in Tris-HCl buffer (10 mM Tris-HCl, pH 8.0, 100 mM KCl and 1 mM $MgCl_2$) for 1 h. Then the solution containing AuNPs-DNA(Dox) conjugates were collected by centrifuged (15,000 rpm, 20 min).

PrP^C mediated drug release

When AuNPs-DNA(Dox) (2 nM) were incubated with PrP^C (0, 20, 50, 100, 200, 400 nM) in Tris-HCl buffer for 1.5 h, Dox was released from DNA into the solution. The amount of released Dox was determined by fluorescence maximum emission wavelength at 562 nm, with excitation at 490 nm. According to the amount of Dox released from AuNPs-DNA(Dox) conjugates, the maximum drug loading was calculated by a fluorescence standard linear calibration curve of Dox, which was generated by using the emission intensity at 562 nm of the known concentrations of Dox (excitation at 490 nm).

In vitro cytotoxicity assay

SK-N-SH cells and A549 cells were respectively cultured in MEM (HyClone) and RPMI-1640 (HyClone), which were both supplemented with 10 % fetal bovine serum (HyClone) at 37 °C under 5 % CO_2. Two kinds of cells were cleaved by trypsin (HyClone) and transferred into two 96-well (10^4 cells / well) tissue culture plates and allowed to grow for 24 h. Then 10 μL 50 nM AuNPs-DNA(Dox), 10 μL 50 nM AuNPS-DNA, and 10 μL 3.8 μM Dox were added into different wells. After 4 h incubation, the solution was removed and fresh medium contain 2% fetal bovine serum was added for further cell growth (24 h). For the cytotoxicity assay, the cells were washed after 24 h, then 90 μL medium and 10 μL CCK-8 were added to each well and incubated for 1 h. The optical densities (OD) of the mixtures were measured with a Microplate Reader Model at 450 nm. The cell viabilities were calculated by comparing AuNPs-DNA(Dox), AuNPs-DNA and Dox treated cells with the untreated cells.

Fluorescence image

A549 cells and SK-N-SH cells were cleaved by trypsin and transferred to two 24-well plates (10^4 cells / well) and allowed to

grow for 24 h. Then 30 μL PBS, 30 μL 10 nM AuNPs-DNA(Dox) and 30 μL 20 nM AuNPs-DNA(Dox) were added into the SK-N-SH cells. 30 μL 10 nM AuNPs-DNA(Dox) was added into the A549 cells. Another group of 30 μL 10 nM AuNPs-DNA(Dox) was incubated with SK-N-SH cells (SK-N-SH cells were pre-treated with AuNPs-DNA for 4 h). The final concentration of AuNPs-DNA(Dox) in SK-N-SH cells were 0, 1 nM and 2 nM, respectively. In A549 cells, the final concentration of AuNPs-DNA(Dox) was 1 nM. After incubation for 4 h, the cells were washed three times with PBS buffer and fixed with 4% paraformaldehyde for 30 min. For investigation the intracellular distribution of Dox, the cells were stained with Hoechst 33258 (0.5 μg/mL), and then mounted on microscope slides for imaging.

Results and discussion

Principle for targeting drug delivery system

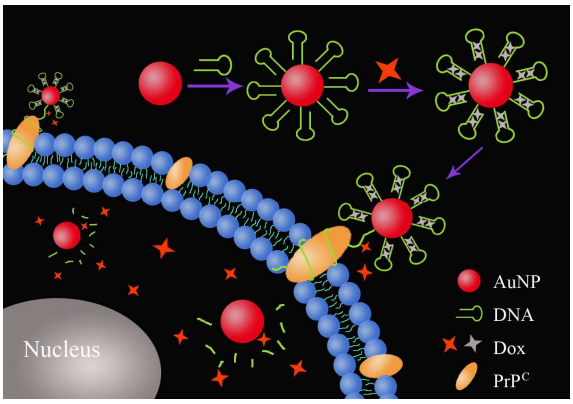

Scheme 1 Schematic procedure for preparation of AuNPs-DNA(Dox) conjugates and PrP^C-mediated Dox release.

Herein, a simple and applicable drug delivery system was designed, which could image and deliver anticancer drug Dox to the target SK-N-SH cells. The operation principle was illustrated in Scheme 1. The system was comprised of three components: AuNPs, DNA and Dox. DNA could form a molecular beacon configuration with two pairs of double-stranded CG sequences in stem region and PrP^C aptamer in loop region. Citrate-coated AuNPs were modified with thiolated DNA that contains PrP^C aptamer to form AuNPs-DNA complexes at first, and then incubated with Dox in buffer solution. The fluorescence of Dox was quenched and the toxicity of Dox was decreased when intercalated in the stem double-stranded CG or GC of DNA. The SK-N-SH cells could overexpress PrP^C, which biologically recognize PrP^C aptamer in AuNPs-DNA(Dox) complexes to improve the intracellular uptake of drug complexes. Some Dox molecules can be released from DNA when recognize with PrP^C and then the toxicity of Dox could be recovered, which increased the drug concentration in local cancer tissues; the other AuNPs-DNA(Dox) complexes further enter into cancer cells by endocytosis, wherein, the nuclease in cells could degrade DNA and release the rest of Dox that can induce cells apoptosis.

The synthesis and characterization of AuNPs-DNA(Dox)

As shown in Fig. 1A, the absorption peak of the as-prepared AuNPs centered at 518 nm, which red-shifted 3 nm when conjugated with DNA. After Dox intercalated in DNA, the absorption of AuNPs-DNA(Dox) showed no difference compared with AuNPs-DNA. It was also found that the AuNPs didn't aggregate after loading drugs as the colors of AuNPs, AuNPs-DNA and AuNPs-DNA(Dox) remained red (Fig. 1B). The hydrated diameter of citrate-stabilized AuNPs, AuNPs-DNA, AuNPs-DNA(Dox) were 23.1 nm, 55.2 nm and 59.4 nm. Furthermore, the zeta potential of AuNPs, AuNPs-DNA and AuNPs-DNA(Dox) were -26.4 mv, -33.4 mv and -30.2 mv, respectively. Both hydrated diameter mesurement and zeta potential result suggesting that the DNA was fixed on AuNPs and the Dox was intercalated in DNA. The morphology of AuNPs didn't change after being functionalized with DNA and loading Dox as shown by the TEM image (Fig. 1C, D, E).

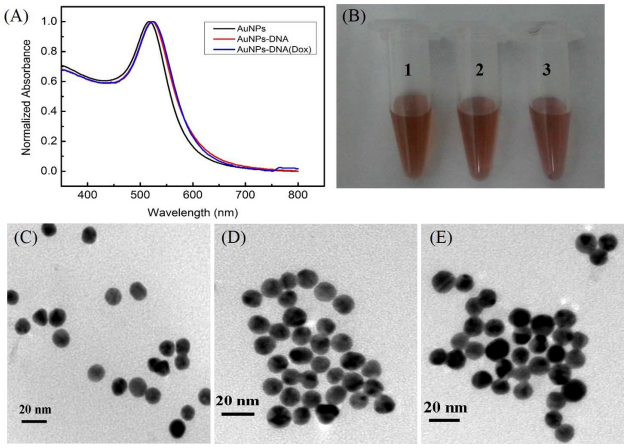

Fig. 1 The characterization of drug carrier. (A) UV-vis absorption spectra of AuNPs, AuNPs-DNA and AuNPs-DNA(Dox). (B) The colors of 1, AuNPs; 2, AuNPs-DNA; 3, AuNPs-DNA(Dox). TEM image of (C) AuNPs, (D) AuNPs-DNA and (E) AuNPs-DNA (Dox).

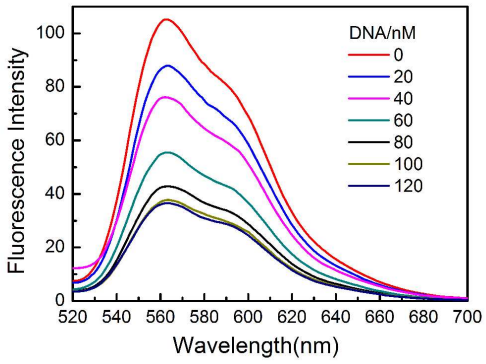

Fig. 2 Fluorescence spectra of Dox solution (200 nM) with increasing molar ratios of DNA, from top to bottom 0, 20, 40, 60, 80, 100, 120 nM.

To determine the loading efficiency of Dox molecules intercalated into the double-stranded CG sequences of DNA, the fluorescence quenching was monitored. As the amount of added DNA increased, a sequential decreases in the fluorescence emission spectra of Dox were observed when the concentration of Dox was fixed at 200 nM (Fig. 2). When the Dox was incubated with 120 nM DNA, the fluorescence intensity showed no obvious difference compared with 100 nM DNA, which demonstrated that 200 nM Dox incubated with 100 nM DNA could ultimately reach

a maximum level of fluorescence quenching. This result suggested that the loading capacity of each DNA was 2 Dox molecules. The DNA we designed has two pairs of "-CG-" in stem, which could load 2 Dox molecules theoretically. The experimental data was consistent with the theoretical value well. AuNPs with excellent biocompatibility and lower toxicity were widely used in bioimage, drug delivery and bioanalysis as vehicles. In this work, we fixed DNA onto the surface of AuNPs with the goals to achieve better biocompatibility and increase the density of Dox that could be selectively and efficiently uptaken by the cells.

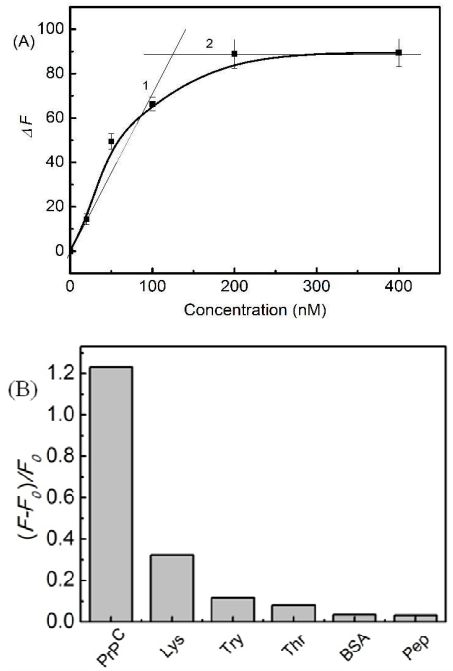

Fig. 3 (A) Fluorescence data for the AuNPs-DNA(Dox) (2 nM) in the presence of various concentration of PrP^C: 0, 20, 50, 100, 200, 400 nM; time, 1.5 h; λ_{ex}, 490 nm; λ_{em}, 562 nm, ΔF represents the fluorescence enhancement value after reaction. (B) Specificity of the PrP^C targeted drug delivery system. PrP^C were 100 nM; lysozyme(Lys), trypsin(Try), bovine serum albumin (BSA), thrombin(Thr) and pepsin(Pep) were all 200 nM. *Fo*, the background fluorescence intensity of AuNPs-DNA(Dox) solution; *F*, the fluorescence intensity of solution after addition of various proteins for 1.5 h.

The release of Dox from AuNPs-DNA(Dox) conjugates was achieved by the biological recognition with PrP^C. The reaction time between AuNPs-DNA(Dox) and PrP^C was optimized to be 1.5 h (Fig. S1). The fluorescence intensity of Dox changed with the increase of PrP^C from 0 to 400 nM was observed (Fig. 3A). When the concentration of PrP^C was increased to 125 nM, the fluorescence intensity of Dox didn't continue increasing, which suggested that 2 nM AuNPs-DNA(Dox) could complete the reaction with 125 nM PrP^C. The fluorescence standard linear equations of Dox was I=0.600c-2.988 (I represented the fluorescence intensity, and c was the concentration of Dox) (Fig. S2). When Dox was released from AuNP-DNA(Dox) completely, the I_{max} = 88, and it could be calculated that $c \approx 152$, which suggested that 2 nM AuNPs-DNA(Dox) released about 152 nM Dox correspond to reaction with 76 nM DNA, so the AuNPs-DNA(Dox) conjugates could load 76 Dox molecules per AuNP, which could be inferred that each AuNP had 38 DNA on its surface. The stability of this AuNPs-DNA(Dox) was investigated in Fig. S3, only a small amount of Dox was released after 30 days in 4 ^oC, which suggested the system of AuNPs-DNA(Dox) was very stable.

To confirm the selectivity of the propoesd strategy, several proteins such as lysozyme, trypsin, thrombin, BSA, pepsin were investigated, even they have different isoelectric points (pI) and structures (Fig. 3B). The results demonstrated that the fluorescence enhancement ratio of AuNPs-DNA(Dox) in the presence of PrP^C was much larger than other proteins showing excellent selectivity toward PrP^C, which was attributed to the specific biological identification between aptamer and PrP^C. While for other proteins, the DNA beacon could not open efficiently to release Dox, so that the fluorescence enhancement ratio was much smaller than the target protein.

Cytotoxicity research

It is very important to investigate the cytotoxicity of vehicles and the efficacy of drug-vehicle conjugates in drug delivery systems, so we evaluated the toxicities of AuNPs-DNA and AuNPs-DNA(Dox) by using the Cell Counting Kit-8 (CCK-8). As shown in Fig. 4, the cell survival of SK-N-SH cells and A549 cells are slightly larger than 100 % after incubated with AuNPs-DNA exhibited no cytotoxicity. It also can be concluded that the toxic effects of AuNPs-DNA(Dox) on SK-N-SH cells and A549 cells are significantly different. The cell viability was 71.1 % for SK-N-SH cells versus 97.4 % for A549 cells. CCK-8 assay revealed that the AuNPs-DNA(Dox) were more cytotoxic toward targeted SK-N-SH cells than non-targeted A549 cells. For free Dox, the viabilities of two cells were nearly the same (64.5 % for SK-N-SH cells and 62.7 % for A549 cells). In addition, the cytotoxic of AuNPs-DNA(Dox) was slightly less than equivalent free Dox, that's probably because a small amount of Dox didn't released from the drug carrier. However, compared with free Dox, this AuNPs-DNA(Dox) achieved a relatively high efficiency of drug release for target.

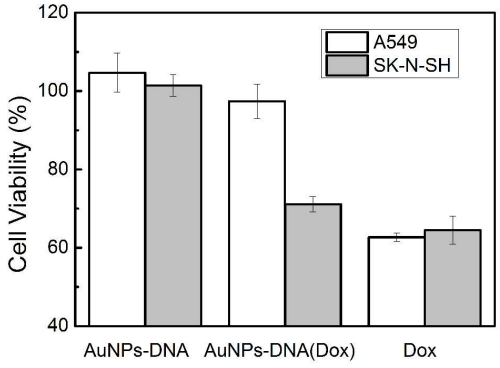

Fig. 4 In vitro cell viability measured by CCK-8 assays. A549 and SK-N-SH cells were incubated with AuNP-DNA (5 nM), AuNP-DNA(Dox) (5 nM) and free Dox (0.38 μM).

Fluorescence imaging

As a small molecular, free Dox is transported into cells by diffusion, while the pattern of AuNPs-DNA(Dox) enter to the SK-N-SH cells is *via* combing to PrP^C of cell surface then

endocytosis by target cells. The specifical binding and release of Dox from AuNPs-DNA(Dox) were further studied by fluorescence imaging. From Fig. 5a-d, it can be observed that, no fluorescence signal was captured in control SK-N-SH cells. As the concentrations of AuNPs-DNA(Dox) increased from 1 nM to 2 nM, more drug was released into the target cells and the fluorescence intensity of intracellular Dox became stronger (Fig. 5e-l). The overlay of DIC, Dox and Hoechst demonstrated that the drug was transported into nuclear successfully.

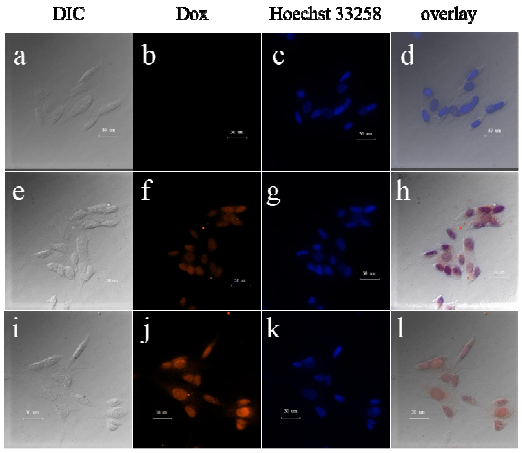

Fig. 5 Fluorescence images of SK-N-SH cells incubated with AuNPs-DNA(Dox) at different concentrations. Differential interference contrast (DIC) (a, e, i), Dox (b, f, j), Hoechst 33258 (c, g, k) and the overlay of fluorescence and DIC (d, h, l). The images a-d showed that no AuNPs-DNA(Dox) was added into SK-N-SH cells; in the images of e-h and i-l, the final concentrations of AuNPs-DNA(Dox) in SK-N-SH cells are 1 nM and 2 nM, respectively. Scale bar, 30 μm.

To confirm the targeting of our drug delivery system, A549 cells that couldn't express PrP^C on their surface were chosen as a control to incubate with AuNPs-DNA(Dox), and AuNPs-DNA was used to pre-treat with SK-N-SH cells for 4h to block the recognition of AuNPs-DNA(Dox) and PrP^C on SK-N-SH cells. As shown in Fig. 6, compared with SK-N-SH cells (c, f), A549 cells (a, d) showed no obvious fluorescence when added the same concentration of AuNPs-DNA(Dox), and a much weaker fluorescence was observed in pre-treated SK-N-SH cells (b, e), suggesting that the targeting drug delivery system of AuNPs-DNA(Dox) was based on the specific identification between aptamer and PrP^C.

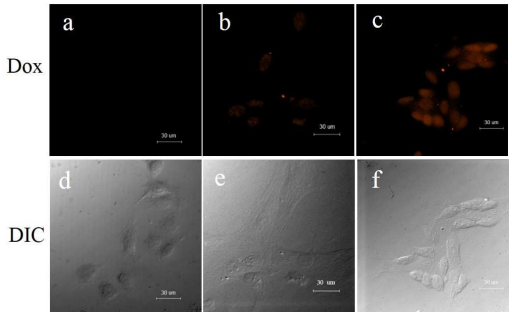

Fig. 6 Fluorescence images of AuNPs-DNA(Dox) incubate with (a,d) A549 cells, (b, e) SK-N-SH cells were pretreated by AuNPs-DNA, (c,f) SK-N-SH cells. The final concentrations of AuNPs-DNA(Dox) in all cells are 1 nM. Scale bar, 30 μm.

Conclusions

In summary, we have reported an AuNPs mediated DNA-Dox conjugate for targeted drug delivery, in which the targeting aptamer ligand and therapeutic drug are incorporated into one platform. Cytotoxicity research and fluorescence imaging results demonstrated that the AuNPs-DNA(Dox) could be successfully realeased in targeted SK-N-SH cells and produce efficiently cytotoxicity to them. However, for non-target cells, such as A549 cells, the drug conjugates couldn't be delivered into cancer cells to kill them. This control experiment indicated that the AuNPs-DNA(Dox) won't yield undesirable side effects to non-target tissues during treatment. It is demonstrated that the AuNPs-DNA(Dox) is a promising anti-cancer drug for the targeted therapeutic of neuroblastoma cancer.

Acknowledgements

This work was financially supported by the National Basic Research Program of China (973 Program, No. 2011CB933600), and Chongqing Program for 100 Outstanding Science and Technology Leading Talents under the direction of Chongqing Science and Technology Commission.

Notes and references

[a] *Key Laboratory of Luminescence and Real-Time Analytical Chemistry (Southwest University), Ministry of Education, College of Pharmaceutical Sciences, Southwest University, 400715 Chongqing, PR China. Fax: +86-23-68866796; Tel: +86-23-68254659; E-mail: chengzhi@swu.edu.cn; wi123456@swu.edu.cn*

[b] *College of Chemistry and Chemical Engineering, Southwest University, 400715 Chongqing, PR China*

† Electronic Supplementary Information (ESI) available: Additional information and figures. See DOI: 10.1039/b000000x/

1. A. Jemal, F. Bray, M. M. Center, J. Ferlay, E. Ward and D. Forman, *CA Cancer J. Clin.*, 2011, **61**, 69-90.
2. M. Ferrari, *Nat. Rev. Cancer*, 2005, **5**, 161-171.
3. I. B. Vasconcelos, T. G. d. Silva, G. C. G. Militao, T. A. Soares, N. M. Rodrigues, M. O. Rodrigues, N. B. d. Costa, R. O. Freire and S. A. Junior, *RSC Adv.*, 2012, **2**, 9437-9442.
4. C. Liu, Z. Zhang, X. Liu, X. Ni and J. Li, *RSC Adv.*, 2013, **3**, 25041-25049.
5. J. Wang, G. Zhu, M. You, E. Song, M. I. Shukoor, K. Zhang, M. B. Altman, Y. Chen, Z. Zhu, C. Z. Huang and W. Tan, *ACS Nano*, 2012, **6**, 5070-5077.
6. W. J. Gradishar, S. Tjulandin, N. Davidson, H. Shaw, N. Desai, P. Bhar, M. Hawkins and J. O'Shaughnessy, *J. Clin. Oncol.* , 2005, **23**, 7794-7803.
7. P. P. Karmali, V. R. Kotamraju, M. Kastantin, M. Black, D. Missirlis, M. Tirrell and E. Ruoslahti, *Nanomedicine*, 2009, **5**, 73-82.
8. Y. Wang, K. Wang, J. Zhao, X. Liu, J. Bu, X. Yan and R. Huang, *J. Am. Chem. Soc.*, 2013, **135**, 4799-4804.
9. D. Pornpattananangkul, L. Zhang, S. Olson, S. Aryal, M. Obonyo, K. Vecchio, C.-M. Huang and L. Zhang, *J. Am. Chem. Soc.*, 2011, **133**, 4132-4139.
10. D. Kim, Y. Y. Jeong and S. Jon, *ACS Nano*, 2010, **4** 3689-3696

11. A. Z. Wang, V. Bagalkot, C. C. Vasilliou, F. Gu, F. Alexis, L. Zhang, M. Shaikh, K. Yuet, M. J. Cima, R. Langer, P. W. Kantoff, N. H. Bander, S. Jon and O. C. Farokhzad, *ChemMedChem*, 2008, **3**, 1311-1315.
12. X. T. Zheng, H. L. He and C. M. Li, *RSC Adv.*, 2013, **3**, 24853-24857.
13. S. Dhar, F. X. Gu, R. Langer, O. C. Farokhzad and S. J. Lippard, *Proc. Natl. Acad. Sci. USA* 2008, **105**, 17356-17361.
14. P. F. Gao, L. L. Zheng, L. J. Liang, X. X. Yang, Y. F. Li and C. Z. Huang, *J. Mater. Chem. B*, 2013, **1**, 3202-3208.
15. W. Pan, H. Yang, T. Zhang, Y. Li, N. Li and B. Tang, *Anal. Chem.*, 2013, **85** 6930-6935.
16. J. M. Rosenholm, E. Peuhu, J. E. Eriksson, C. Sahlgren and M. Lindén, *Nano Lett.*, 2009, **9**, 3308-3311.
17. X. Yang, Y. Wang, X. Huang, Y. Ma, Y. Huang, R. Yang, H. Duan and Y. Chen, *J. Mater. Chem.*, 2011, **21**, 3448-3454.
18. B. M. Barth, E. I. Altinoğlu, S. S. Shanmugavelandy, J. M. Kaiser, D. Crespo-Gonzalez, N. A. DiVittore, C. McGovern, T. M. Goff, N. R. Keasey, J. H. Adair, T. P. Loughran, D. F. Claxton and M. Kester, *ACS Nano*, 2011, **5**, 5325-5337.
19. Morishita M and P. NA, *Drug Discovery Today*, 2006, **11**, 905-910.
20. J. M. Hooker, J. P. O'Neil, D. W. Romanini, S. E. Taylor and M. B. Francis, *Mol Imaging Biol*, 2008, **10**, 182-191.
21. C. Moon, Y. M. Kwon, W. K. Lee, Y. J. Park and V. C. Yang, *J. Controlled Release*, 2007, **124**, 43-50.
22. S. S. Dharap, Y. Wang, P. Chandna, J. J. Khandare, B. Qiu, S. Gunaseelan, P. J. Sinko, S. Stein, A. Farmanfarmaian and T. Minko, *Proc. Natl. Acad. Sci. USA*, 2005, **102**, 12962-12967.
23. G. Qiao, L. Zhuo, Y. Gao, L. Yu, N. Li and B. Tang, *Chem. Commun*, 2011, **47**, 7458-7460.
24. T. Chen, M. I. Shukoor, Y. Chen, Q. Yuan, Z. Zhu, Z. Zhao, B. Gulbakan and W. Tan, *Nanoscale*, 2011, **3**, 546-556.
25. Y.-F. Huang, D. Shangguan, H. Liu, J. A. Phillips, X. Zhang, Y. Chen and W. Tan, *ChemBioChem*, 2009, **10**, 862 - 868.
26. P. P. Hu, L. Q. Chen, C. Liu, S. J. Zhen, S. J. Xiao, L. Peng, Y. F. Lia and C. Z. Huang, *Chem. Commun.*, 2010, **46**, 8285-8287.
27. G. García-Santos, I. Antolín, F. Herrera, V. Martín, J. Rodriguez-Blanco, M. d. P. Carrera and C. Rodriguez, *J. Pineal Res.* , 2006, **41**, 130-135.
28. S. J. Xiao, P. P. Hu, X. D. Wu, Y. L. Zou, L. Q. Chen, L. Peng, J. Ling, S. J. Zhen, L. Zhan, Y. F. Li and C. Z. Huang, *Anal. Chem.*, 2010, **82**, 9736-9742.
29. L. Q. Chen, S. J. Xiao, P. P. Hu, L. Peng, J. Ma, L. F. Luo, Y. F. Li and C. Z. Huang, *Anal. Chem.*, 2012, **84**, 3099-3110.
30. Vaishali Bagalkot, Omid C. Farokhzad, Robert Langer and S. Jon, *Angew. Chem. Int. Ed.*, 2006, **45**, 8149–8152.
31. C. Li, T. Chen, I. Ocsoy, G. Zhu, E. Yasun, M. You, C. Wu, J. Zheng, E. Song, C. Z. Huang and W. Tan, *Adv. Funct. Mater.*, 2014, 1772-1780.
32. R. Elghanian, J. J. Storhoff, R. C. Mucic, R. L. Letsinger and C. A. Mirkin, *Science*, 1997, **277**, 1078-1081.
33. J. Li, H. E. Fu, L. J. Wu, A. X. Zheng, G. N. Chen and H. H. Yang, *Anal. Chem.*, 2012, **84**, 5309-5315.
34. J. Liu and Y. Lu, *Nat. Protoc.*, 2006, **1**, 246-253.
35. P. Fan, A. K. Suri, R. Fiala, D. Live and D. J. Patel, *J. Mol. Biol.*, 1996, **258**, 480-500.